ATMOSPHERIC SCIENCE LETTERS
Atmos. Sci. Let. **16**: 177–183 (2015)
Published online 6 February 2015 in Wiley Online Library
(wileyonlinelibrary.com) **DOI:** 10.1002/asl2.562

RMetS
Royal Meteorological Society

Moisture sources of an extreme precipitation event in Sichuan, China, based on the Lagrangian method

Yongjie Huang[1,2]* and Xiaopeng Cui[1,3]

[1]*Key Laboratory of Cloud-Precipitation Physics and Severe Storms (LACS), Institute of Atmospheric Physics, Chinese Academy of Sciences, Beijing, China*
[2]*College of Earth Science, University of Chinese Academy of Sciences, Beijing, China*
[3]*Collaborative Innovation Center on Forecast and Evaluation of Meteorological Disasters, Nanjing University of Information Science and Technology, China*

**Correspondence to:*
Y. Huang, Key Laboratory of Cloud-Precipitation Physics and Severe Storms (LACS), Institute of Atmospheric Physics, Chinese Academy of Sciences, Beijing 100029, China.
E-mail: huangyj@mail.iap.ac.cn

Received: 30 May 2014
Revised: 1 December 2014
Accepted: 6 January 2015

Abstract

In July 2013, an extreme precipitation event occurred in Sichuan, China, causing severe flooding, debris flows, and substantial losses. Moisture sources and transport of this event and quantification of the contribution from moisture sources were studied using the Lagrangian method. The results show that the vast majority of particles influencing this event originated from the relatively lower troposphere south of the precipitation region and can be traced back to the Arabian Sea. Moreover, the total moisture from the source regions accounts for more than 80% of the precipitation; moisture originating from the India Peninsula–Bay of Bengal–Indo-China Peninsula region had the highest contribution.

Keywords: moisture sources; extreme precipitation event; Lagrangian method; Sichuan; FLEXPART

1. Introduction

Extreme precipitation is a main cause of severe natural disasters, particularly in Sichuan, where the terrain is complex. Heavy precipitation, which can cause flooding, debris flows, landslides, and other natural disasters, is a severe threat to lives and property and poses a high challenge to weather forecasters in mountainous regions. Perhaps the most puzzling question is the origin of the water vapor that produces such precipitation (Stohl and James, 2004). Therefore, it is crucial to study water vapor source regions and moisture transport processes for strong precipitation (Newell *et al.*, 1992). In general, several possible moisture sources for precipitation have been identified, such as water vapor already present in the atmosphere over the region, water vapor advected into the region by wind, and local evaporation from the land surface of the region (Brubaker *et al.*, 1993). However, questions remain in determining which type of moisture source is the most important and the respective contributions of each type for the precipitation. The answers to these questions are very important for the study of extreme precipitation events.

Several methods are used to identify moisture source regions that contribute to precipitation and the moisture transport paths involved. Although isotopic analysis is one such technique (Weyhenmeyer *et al.*, 2002; Bonne *et al.*, 2014), it is impossible to examine past events for which no rain samples are available (Gustafsson *et al.*, 2010). Many previous studies have used vertically integrated moisture flux to estimate the moisture sources and transport for the precipitation (Xu *et al.*, 2003; Zhou *et al.*, 2005; Holman and Vavrus, 2012). However, due to the fast transition of wind fields, this Eulerian method gives only simple moisture transport paths and fails to provide information on the geographical sources of the moisture (Sodemann *et al.*, 2008; Drumond *et al.*, 2011b). Further, an additional sophisticated method, the Lagrangian method, has been developed to quantify the moisture transport (Stohl and James, 2004, 2005) and is widely applied in the studies of moisture sources (Stohl *et al.*, 2008; Sodemann and Stohl, 2009; Gimeno *et al.*, 2010a, 2010b; Drumond *et al.*, 2011a; Chen *et al.*, 2013; Gimeno *et al.*, 2013; Gómez-Hernández *et al.*, 2013).

This study examines an extreme precipitation event that occurred on 8–11 July 2013. This event led to widespread flooding, landslides, and debris flows that caused considerable infrastructure damage and numerous fatalities. At least 58 people died, 175 others were reported missing, and an estimated 6 million lives were disrupted as a result of the rainstorm-triggered floods and landslides (http://en.wikipedia.org/wiki/2013_Southwest_China_floods). In this study, a Lagrangian model known as the flexible particle dispersion model (FLEXPART) is used for examining the moisture transport, identifying the main moisture source regions, and quantifying the contribution from moisture source regions associated with the precipitation.

2. Model and methodology

2.1. Model description

To determine the main moisture sources and their contributions for the target region of the extreme precipitation, we used of the FLEXPART model, which was developed by Stohl and James (2004, 2005). To increase the reliability of results, FLEXPART 9.02 was integrated using two types of datasets. The first includes the final version of the National Centers for Environmental Prediction (NCEP FNL) Operational Global Analysis data available every 6 h with a $1^\circ \times 1^\circ$ resolution on 26 vertical levels (http://rda.ucar.edu/datasets/ds083.2/). The second includes NCEP Climate Forecast System Version 2 (NCEP–CFSv2) 6-h forecast data, including land cover, temperature, relative humidity, and three-dimensional wind, in 37 levels with a resolution of $0.5^\circ \times 0.5^\circ$ (http://rda.ucar.edu/datasets/ds094.0/). FLEXPART was run in the region (40°–160°E, 10°S–60°N) using the domain filling mode, with a total of 1.2 million particles released for driving data of both NCEP FNL and NCEP–CFSv2. The modeling periods were both from 0000 UTC 1 July 2013 to 0000 UTC 12 July 2013. The model outputs were recorded every 3 h and included the identity number of particles, three-dimensional position (latitude, longitude, and altitude), temperature, specific humidity, air density, atmospheric boundary layer height and tropopause height at the positions of particles, and the mass of each particle.

2.2. Methodology

2.2.1. Target particles

Using the Lagrangian analysis method, we can track only target particles making important contributions to precipitation process, identify sites in which the water vapor of the target particles increases, and finally determine the moisture source regions of the precipitation. In our study, we used a similar method applied by Chen *et al.* (2011) to determine target particles that have a significant effect on the precipitation process in the precipitation period. We then tracked these target particles and analyzed their contributions to the precipitation. This identification process of the target particles includes the following main steps:

1. According to the precipitation period, determine period for selection of target particles: 0000 UTC 8 July 2013 to 0000 UTC 11 July 2013.
2. According to the precipitation distribution, determine the precipitation target region: 27°–35°N, 99°–107°E.
3. Among the particles selected in steps (a) and (b), find the particles with grid precipitation larger than 2 mm. The precipitation data used here are hourly precipitation observed by automatic weather stations in China merged with CMORPH satellite data with a $0.1^\circ \times 0.1^\circ$ resolution (Pan *et al.*, 2012; Shen *et al.*, 2013).
4. Among the particles selected in step (c), find the particles in which the 3 h specific humidity change is less than $-1\ \mathrm{g\,kg^{-1}}$.

By following the above process, we obtained the target particles with high contribution to the precipitation. However, because we ignored some particles that had minor effects on the precipitation, the target particles generated may amount to less than the actual precipitation.

2.2.2. Identification of moisture source regions and quantification of contribution

In the Lagrangian method, changes in specific humidity q with time t are used to diagnose the water vapor content of a particle (Stohl and James, 2004, 2005),

$$e - p = m\frac{\mathrm{d}q}{\mathrm{d}t} \tag{1}$$

where m is the mass of the particle, and e and p are the rates of moisture increases and decreases along the trajectory, respectively. Amassing the moisture changes of all N particles residing in the atmospheric column over an area A gives

$$E - P \approx \frac{\sum_{i=1}^{N}(e-p)}{A} = \frac{\sum_{i=1}^{N} m\frac{\mathrm{d}q}{\mathrm{d}t}}{A} \tag{2}$$

where E–P is the surface freshwater flux, and E and P are the evaporation and precipitation rates unit area, respectively. From the FLEXPART output, changes in q with time t could be integrated to diagnose E–P. However, in the same location in a very short-time interval, there is always only one dominant process, either evaporation or precipitation (Trenberth *et al.*, 2003). Therefore, under certain assumptions, we can diagnose E or P individually, instantaneous rates of evaporation $E \approx E-P$ when $E-P > 0$, or precipitation $P \approx P-E$ when $E-P < 0$ (Stohl and James, 2004, 2005). When we diagnose strong precipitation events, a separation of E and P is reasonable to identify the moisture source regions of the precipitation. A region with a high positive E–P value indicates that it may be a strong moisture source for the precipitation, and target particles passing over this region may carry moisture into the target region. It is shown that the Lagrangian method (Equation (2)) can track E–P forward or backward in time by evaluating (Equation (1)) along the trajectories of selected particles, which is the main advantage of the Lagrangian method over the Eulerian method (Stohl and James, 2004, 2005).

However, before precipitation occurs, air parcels may undergo multiple cycles of evaporation and precipitation from the examined sources along their way to the target region. Therefore, because of precipitation during particle transportation, earlier evaporative sources of moisture will contribute less to the precipitation in

the target region (Sodemann *et al.*, 2008). Hence, we should consider the continuous change in moisture of the target particles along their trajectories to the precipitation in the target region. Sodemann *et al.* (2008) introduced a source attribution method for calculating the contribution of each evaporation location along a trajectory to the precipitation at the target location. This method has been widely applied (Stohl *et al.,* 2008; Gimeno *et al.,* 2010a; Chen *et al.,* 2011; Martius *et al.,* 2013). Sun and Wang (2014) made a few alterations to this method and introduced their method as an areal source-receptor attribution method for estimating the contribution of moisture source regions to the precipitation target region. We used this altered method in this study; further details on the areal source-receptor attribution method appear elsewhere (Sun and Wang, 2014).

3. Results

3.1. Precipitation distribution

Figure 1 shows accumulated precipitation of observation and the FLEXPART diagnosis in Sichuan from 0000 UTC 8 July 2013 to 0000 UTC 11 July 2013. The figure shows that strong observation precipitation characterized by southwest–northeast distribution was mainly distributed east of the Tibetan Plateau near steep terrain (Figure 1(a)). The maximum accumulated observation precipitation was more than 400 mm (Figure 1(a)). The diagnosis precipitation based on the outputs of FLEXPART driven by NCEP–CFSv2 data (Figure 1(b)) covered the area of precipitation studied here, and the rain band was also distributed southwest–northeast near the steep terrain east of the Tibetan Plateau. However, the maximum precipitation center was slightly southward of that in the observation precipitation, and the maximum rainfall was slightly weaker. The diagnosis precipitation based on the outputs of FLEXPART driven by NCEP FNL data (Figure 1(c)) showed a precipitation distribution similar to that of the observation precipitation; however, its rainfall intensity was weaker than that of observation. One reason for this discrepancy is that particles having a strong contribution to precipitation were selected as target particles in this study, as discussed in Section 2.2.1. Overall, observation and FLEXPART diagnosis precipitation were consistent in terms of distribution pattern and magnitude of precipitation, although some differences were noted in the specific values of precipitation (Figure 1). Therefore, it can be inferred that the results diagnosed using the Lagrangian method have a high reliability.

3.2. Moisture transport

Figure 2(a) and (b) shows the trajectories for the target particles selected in Section 2.2.1 from 0300 UTC 1 July 2013 to 0000 UTC 11 July 2013, which were simulated by FLEXPART. The trajectory segments are color-coded in the figures according to the associated altitudes. The unit of altitude used here is meters above ground level (AGL) rather than meters above mean sea level (MSL). As shown in the figures, the results are very close between the FLEXPART model simulations driven by NCEP–CFSv2 and NCEP FNL data. The outcome indicates that the vast majority of target particles influencing the precipitation originated south of the target region and can be traced back to the Bay of Bengal, the Arabian Sea, and the Somali Peninsula. Moreover, most of the particles are from relatively lower atmospheric layers below 4000 m AGL. In addition, a small part of the target particles reached the target region from the middle and lower atmospheric layers north of the Tibet Plateau. Few target particles came from eastern China and the South China Sea (Figure 2(a) and (b)). Figure 2(a) and (b) also shows that target particles were transported into target region before ascending and then forming an anticyclonic spin at the high altitude.

To further explain the moisture transport, Figure 2(c) and (d) shows the vertically integrated moisture flux from the surface to 700 hPa ($-g^{-1}\int_{P_s}^{700} q\mathbf{v}\mathrm{d}p$, where g is the acceleration of gravity, q is the specific humidity, P_s is the surface pressure, and $\mathbf{v}$ is the horizontal wind vector) and geopotential height at the 500 hPa mean from 0000 UTC 1 July 2013 to 0000 UTC 11 July 2013, calculated from NCEP-CFSv2 and NCEP FNL data. The figures show that a band of strong moisture flux started from the Arabian Sea, and was then transported through the Indian Peninsula, the Bay of Bengal, and the Indo-China Peninsula before finally reaching the target region. Weak moisture fluxes were transported along the path north of the Tibetan Plateau to reach the target region. Regarding the water vapor fluxes from eastern China and the South China Sea, the subtropical high located over the East China Sea and moisture fluxes from the South China Sea were mainly transported to eastern China and were rarely delivered to the Sichuan region. These results are consistent with the above diagnostic results of the Lagrangian method.

Overall, the above results imply that moisture from the south may have played a key role in this extreme precipitation event; however, its role in the moisture supply requires further analysis.

3.3. Moisture source regions and quantification of contribution

To identify the moisture source regions of the strong precipitation, Figure 3(a) and (b) shows the sum $E-P$ diagnosed from trajectories of the target particles selected in Section 2.2.1 integrated from 0300 UTC 1 July 2013 to 0000 UTC 8 July 2013. The blue areas in the figures represent moisture sinks that include a net release of moisture, and the red areas represent moisture sources that include a net uptake of moisture. From the figures, it is evident that most of the target particles underwent multiple cycles of evaporation and precipitation before reaching the target region of the precipitation. In particular, target particles have

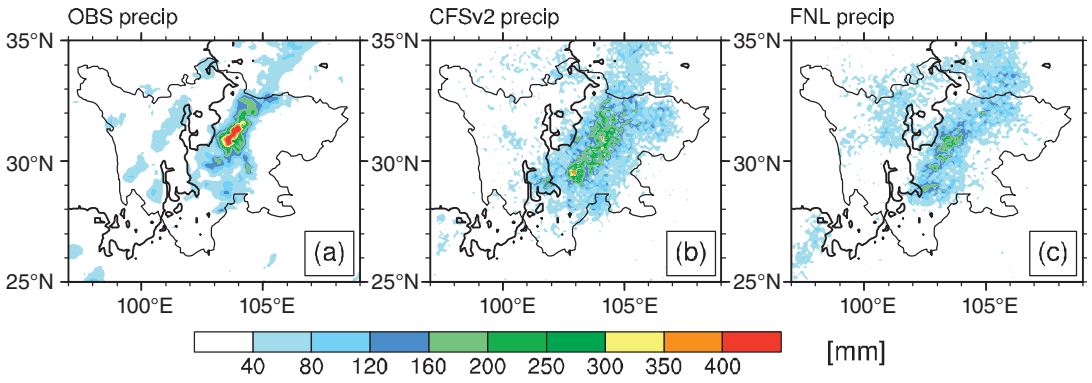

Figure 1. Accumulated precipitation in Sichuan, China, from 0000 UTC 8 July 2013 to 0000 UTC 11 July 2013 (color shading, units: mm). (a) Observation precipitation, (b) and (c) diagnoses based on the outputs from the flexible particle dispersion model (FLEXPART) driven by data from the National Centers for Environmental Prediction Climate Forecast System Version 2 (NCEP–CFSv2) and its final version (NCEP FNL), respectively. Thick solid lines indicate 3 km height contours of the Tibetan Plateau.

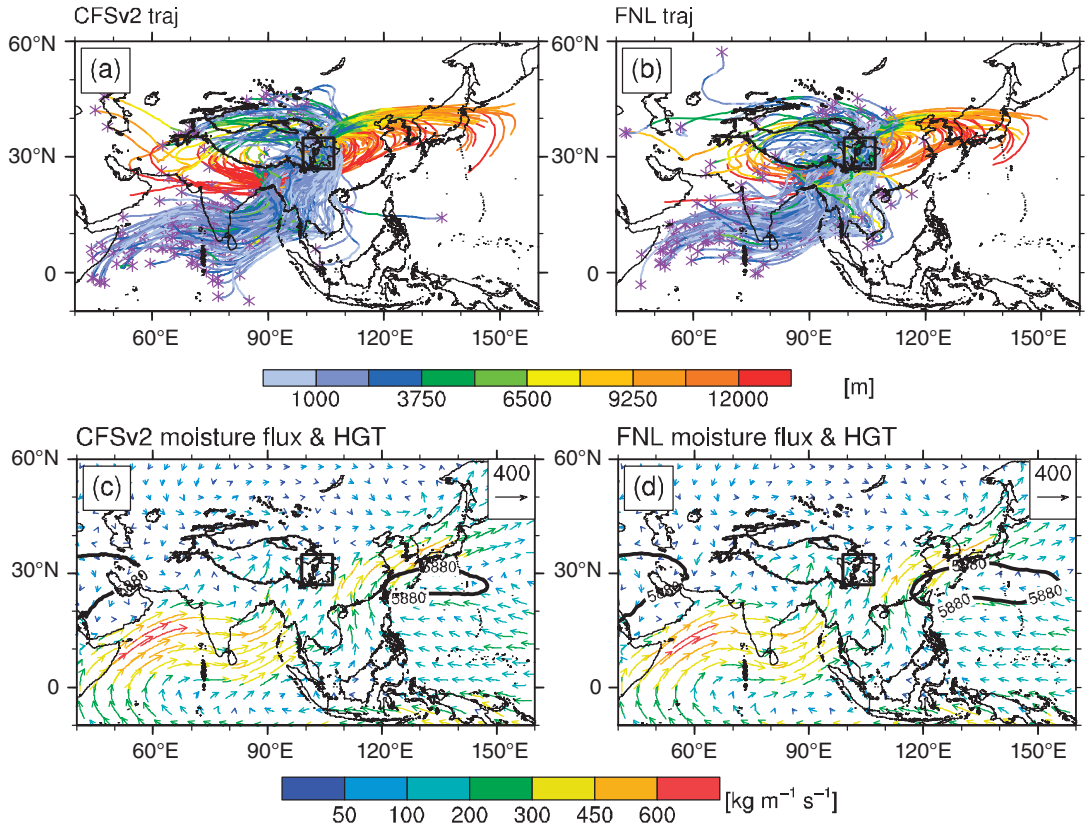

Figure 2. Trajectories for the target particles from 0300 UTC 1 July 2013 to 0000 UTC 11 July 2013, simulated by the flexible particle dispersion model (FLEXPART) driven by data from (a) the National Centers for Environmental Prediction Climate Forecast System Version 2 (NCEP-CFSv2) and (b) its final version (NCEP FNL) and vertically integrated moisture flux from the surface to 700 hPa and geopotential height at 500 hPa mean from 0000 UTC 1 July 2013 to 0000 UTC 11 July 2013, calculated from (c) NCEP-CFSv2 data and (d) NCEP FNL data. Trajectory segments are color-coded according to the associated altitudes above ground level (AGL; units: m). Purple '*' marks in (a) and (b) indicate the beginning of the trajectories. For clarity of presentation, only one trajectory is selected randomly by every 30-target particles. Arrows in (c) and (d) are color-coded according to the magnitude of the moisture flux (units: kg m^{-1} s^{-1}). Thick solid contours in (c) and (d) indicate geopotential height at 500 hPa (units: gpm). Thin solid lines indicate 3 km height contours of the Tibetan Plateau; black rectangles indicate the target regions.

significant net uptakes of moisture through the Arabian Sea and the Bay of Bengal. In addition, the northeast edge of the Tibet Plateau and the target region also have net uptakes of water vapor (Figure 3(a) and (b)). However, when particles were transported from ocean to land, such as those landing at the west coasts of the India Peninsula and Indo-China Peninsula (blue areas in the figures), they exhibited significant net releases of moisture, indicating significant precipitation. Moreover, a strong moisture release region was noted at the southern margin of the Tibetan Plateau near the Hengduan Mountains.

To quantitatively estimate the contribution of the different moisture source regions to precipitation in the

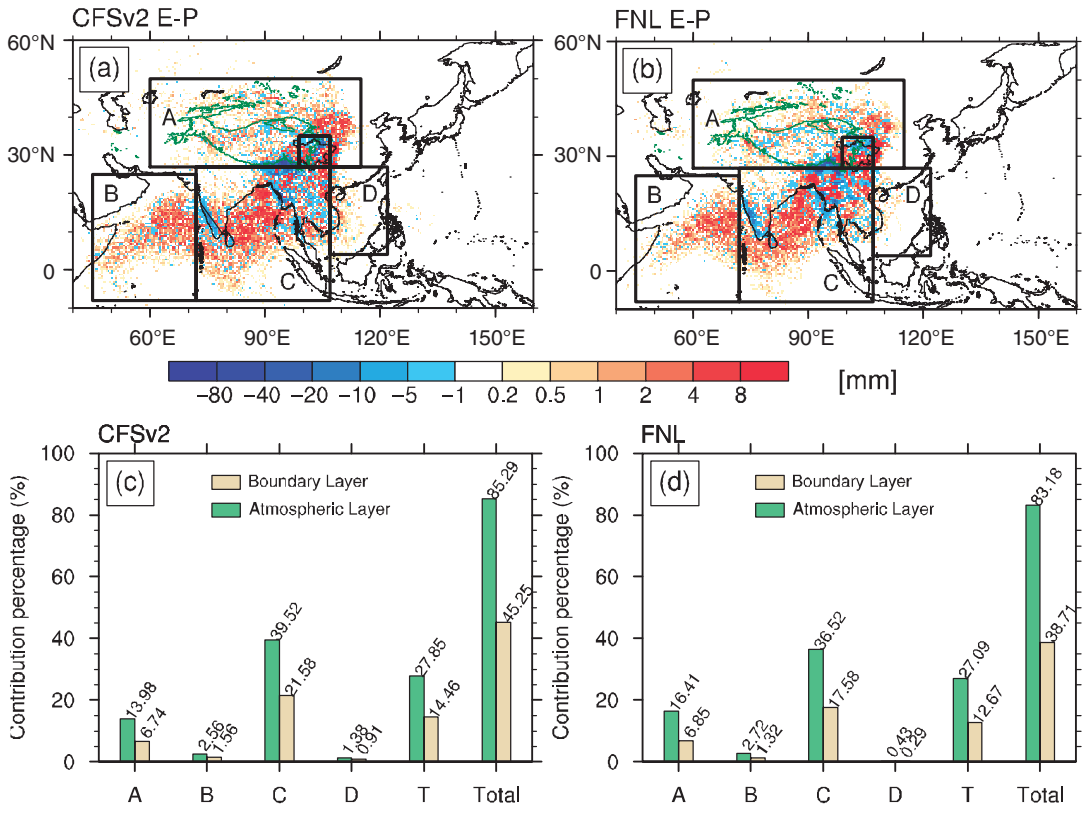

Figure 3. Values of *E*−*P* (units: mm) diagnosed from trajectories of the target particles selected in Section 2.2.1 integrated from 0300 UTC 1 July 2013 to 0000 UTC 8 July 2013, simulated by the flexible particle dispersion model (FLEXPART) driven by data from (a) the National Centers for Environmental Prediction Climate Forecast System Version 2 (NCEP-CFSv2) and (b) its final version (NCEP FNL) and contribution (units: %) of each examined moisture source region shown in (a) and (b) to the total moisture released in the target region (indicated by T). The green solid lines in (a) and (b) indicate 3 km height contours of the Tibetan Plateau. A, B, C, and D indicate the Tibet Plateau and central China region, the Arabian Sea region, the India Peninsula–Bay of Bengal–Indo-China Peninsula region, and the South China Sea region, respectively. T in (c) and (d) indicates the local precipitation target region.

target region, all of the examined regions are denoted by polygons on maps shown in Figure 3(a) and (b), in which A, B, C, and D, indicate the Tibetan Plateau and central China region, the Arabian Sea region, the India Peninsula–Bay of Bengal–Indo-China Peninsula region, and the South China Sea region, respectively. We used the areal source-receptor attribution method to determine the contribution of the moisture source regions to the total release in the precipitation target region, as shown in Figure 3(c) and (d). In addition, the contribution of local evaporation in the target region was also estimated, as indicated in the figures by T. Here, the moisture source contribution both below the boundary layer height and in the entire atmospheric layer was calculated. As shown in the figures, the results of FLEXPART driven by NCEP–CFSv2 data (Figure 3(c)) are consistent with those driven by NCEP FNL data (Figure 3(d)); thus, only the results from the former are discussed here. Figure 3(c) indicates that region C was the moisture source region making the largest contribution to the precipitation, which is mainly the Bay of Bengal, and its contributions of moisture in the entire atmospheric layer and within the boundary layer height to the precipitation in the target region were 39.52 and 21.58%, respectively. The contribution of local evaporation ranked second, and moisture in the entire atmospheric layer and within the boundary layer height of region A, including the Tibet Plateau and central China, respectively, accounted for 13.98 and 6.74% of the precipitation in the target region. The minimum contribution region was D, the South China Sea region, which is consistent with the above analysis.

It is worth noting that although particles had significant net uptakes of moisture through the Arabian Sea (Figure 3(a) and (b)), the moisture contribution to the precipitation in the target region was insignificant because of significant loss en route, such as that caused by landing in the India Peninsula and Indo-China Peninsula. Finally, the total moisture from all examined moisture source regions in the entire atmospheric layer and in the boundary layer accounted for 85.29 and 45.25% of the precipitation in the target region, respectively. The sources of the remaining 14.71% of moisture were unable to be identified in this study; this moisture may have been present in the air particles before the earliest uptake identified, such as before 0300 UTC on 1 July 2013, and not all of moisture source regions have been considered in this study, such as the Eastern China and the East China Sea.

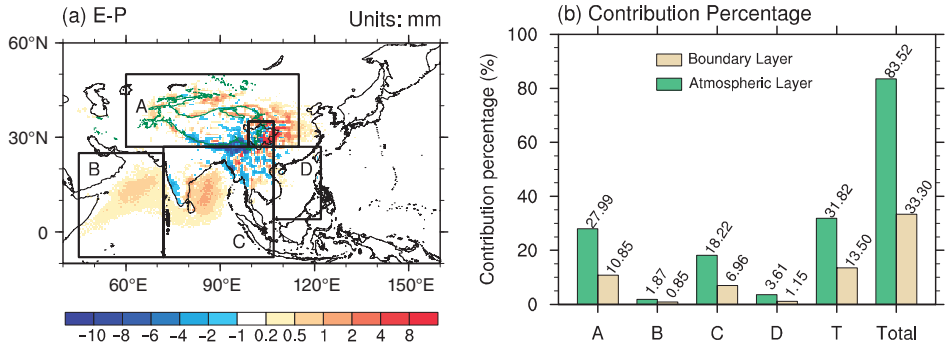

Figure 4. Values of *E*−*P* (units: mm) diagnosed from 10-day trajectories of the air particles during June−September of 2009−2013 simulated by the flexible particle dispersion model (FLEXPART) driven by NCEP FNL data (a), and contribution (units: %) of each examined moisture source region shown in (a) to the total moisture released in the target region (indicated by T). The green solid lines in (a) indicate 3 km height contours of the Tibetan Plateau. A, B, C, and D indicate the Tibet Plateau and central China region, the Arabian Sea region, the India Peninsula−Bay of Bengal−Indo-China Peninsula region, and the South China Sea region, respectively. T in (b) indicates the local target region.

To compare significant moisture sources of the extreme precipitation event in the target region with the climatology of this region, FLEXPART was run forward in time for the period of 2009−2013, and used to backtrack air particles entering the target region for 10-day period during June to September (warm season), 2009−2013.

Figure 4 shows distribution of mean 10-day integrated *E*−*P* during June−September of 2009−2013 (Figure 4(a)), and contribution percentage of each examined moisture source region (shown in Figure 4(a), and same as those in Figure 3(a) and (b)) to the total moisture released in the target region. Comparing Figures 3 and 4, air particles have similar moisture sources and sinks on their way to the target region during either this extreme event or warm season of 2009−2013, while values of the net moisture uptake or release during the extreme precipitation event are relatively larger (Figures 3(a) and (b) and 4(a)). However, contribution of each examined moisture source region to the total moisture released in the target region is significantly different between those of the extreme event and climatology. As for climatology, the local target region was the moisture source region making the largest contribution to the total moisture released in the target region, and the contribution of region A ranked second (Figure 4(b)). Whereas, contribution of region C, which ranked first in the extreme event, was in the third place during June to September of 2009−2013.

Overall, the moisture originating from region C, the India Peninsula−Bay of Bengal−Indo-China Peninsula region, was found to make key contributions to the strong precipitation in the target region.

4. Conclusions

In this study, we used the FLEXPART Lagrangian particle dispersion model with the domain filling mode to examine the moisture sources and transport of an extreme precipitation event occurring in July 2013 in Sichuan, China, which produced flooding and debris flows and caused considerable infrastructure damage and numerous fatalities. In addition, quantification of the contribution from moisture sources was also conducted. To increase the reliability of the conclusions, two types of datasets, NCEP-CFSv2 and NCEP FNL, were used to driven the FLEXPART model. Through comparative analysis, we determined that results from the two model output datasets are highly consistent; therefore, it can be inferred that the results diagnosed using the Lagrangian method have a high reliability. Our major findings are summarized in the following points:

1. The FLEXPART diagnosis precipitation was consistent with observation precipitation in terms of distribution pattern and magnitude of precipitation, although some differences were noted in the specific values of precipitation. Therefore, the diagnosis results in our study have a high reliability.
2. Through analysis of three-dimensional backtracked trajectories of target particles having significant contributions to the heavy rainfall, we determined that the vast majority of target particles influencing the precipitation originated from the relatively lower atmospheric layers south of the target region and can be traced back to the Bay of Bengal, the Arabian Sea, and the Somali Peninsula. Moreover, there was a small part of the target particles coming from middle and lower atmospheric layers along the path north of the Tibetan Plateau, and few target particles came from eastern China and the South China Sea. Analysis of moisture flux verified the above results.
3. Quantification of the contribution of moisture sources indicated that the total moisture from all examined moisture source regions accounted for more than 80% of the precipitation in the target region and that moisture originating from the India Peninsula−Bay of Bengal−Indo-China Peninsula region made key contributions to this strong precipitation, whereas it ranked third in climatology, following that from the local target region and the Tibet Plateau−central China region.

Previous studies have shown that the type of extreme precipitation discussed in this study is very typical in summer in the Sichuan region, where debris flows, landslides, and other secondary geological disasters occur frequently. Thus, although only one event has been analyzed in this article, the conclusions may be representative. In future work, we will conduct composite analysis of multiple extreme precipitation events in Sichuan region to make the conclusions more robust and statistically significant.

Acknowledgements

This work was supported by the Key Research Program of the Chinese Academy of Sciences (Grant No. KZZD-EW-05-01), the National Basic Research Program of China (973 Program) (Grant No. 2014CB441402), and the National Natural Science Foundation of China (Grant No. 41475100). The authors thank Bo Sun, Bin Chen, and Bo Liu for model discussion. They also thank the anonymous reviewers who provided helpful comments that improved the article.

References

Bonne JL, Masson-Delmotte V, Cattani O, Delmotte M, Risi C, Sodemann H, Steen-Larsen HC. 2014. The isotopic composition of water vapour and precipitation in Ivittuut, southern Greenland. *Atmospheric Chemistry and Physics* **14**: 4419–4439.

Brubaker KL, Entekhabi D, Eagleson PS. 1993. Estimation of continental precipitation recycling. *Journal of Climate* **6**: 1077–1089.

Chen B, Xu XD, Shi XH. 2011. Estimating the water vapor transport pathways and associated sources of water vapor for the extreme rainfall event over east of China in July 2007 using the Lagrangian method. *Acta Meteorologica Sinica* **69**: 810–818 (in Chinese).

Chen B, Xu XD, Zhao TL. 2013. Main moisture sources affecting lower Yangtze River Basin in boreal summers during 2004–2009. *International Journal of Climatology* **33**: 1035–1046.

Drumond A, Nieto R, Gimeno L. 2011a. Sources of moisture for China and their variations during drier and wetter conditions in 2000–2004: a Lagrangian approach. *Climate Research* **50**: 215–225.

Drumond A, Nieto R, Hernandez E, Gimeno L. 2011b. A Lagrangian analysis of the variation in moisture sources related to drier and wetter conditions in regions around the Mediterranean Basin. *Natural Hazards and Earth System Sciences* **11**: 2307–2320.

Gimeno L, Drumond A, Nieto R, Trigo RM, Stohl A. 2010a. On the origin of continental precipitation. *Geophysical Research Letters* **37**: L13804, doi: 10.1029/2010gl043712.

Gimeno L, Nieto R, Trigo RM, Vicente-Serrano SM, Lopez-Moreno JI. 2010b. Where does the Iberian Peninsula moisture come from? An answer based on a Lagrangian approach. *Journal of Hydrometeorology* **11**: 421–436.

Gimeno L, Nieto R, Drumond A, Castillo R, Trigo R. 2013. Influence of the intensification of the major oceanic moisture sources on continental precipitation. *Geophysical Research Letters* **40**: 1443–1450, doi: 10.1002/Grl.50338.

Gómez-Hernández M, Drumond A, Gimeno L, Garcia-Herrera R. 2013. Variability of moisture sources in the Mediterranean region during the period 1980–2000. *Water Resources Research* **49**: 6781–6794.

Gustafsson M, Rayner D, Chen DL. 2010. Extreme rainfall events in southern Sweden: where does the moisture come from? *Tellus Series A-Dynamic Meteorology and Oceanography* **62**: 605–616.

Holman KD, Vavrus SJ. 2012. Understanding simulated extreme precipitation events in Madison, Wisconsin, and the role of moisture flux convergence during the late twentieth and twenty-first centuries. *Journal of Hydrometeorology* **13**: 877–894.

Martius O, Sodemann H, Joos H, Pfahl S, Winschall A, Croci-Maspoli M, Graf M, Madonna E, Mueller B, Schemm S, Sedlacek J, Sprenger M, Wernli H. 2013. The role of upper-level dynamics and surface processes for the Pakistan flood of July 2010. *Quarterly Journal of the Royal Meteorological Society* **139**: 1780–1797.

Newell RE, Newell NE, Zhu Y, Scott C. 1992. Tropospheric rivers – a pilot-study. *Geophysical Research Letters* **19**: 2401–2404.

Pan Y, Shen Y, Yu JJ, Zhao P. 2012. Analysis of the combined gauge-satellite hourly precipitation over China based on the OI technique. *Acta Meteorologica Sinica* **70**: 1381–1389. (in Chinese).

Shen Y, Pan Y, Yu JJ, Zhao P, Zhou ZJ. 2013. Quality assessment of hourly merged precipitation product over China. *Transactions of Atmospheric Sciences* **36**: 37–46. (in Chinese).

Sodemann H, Stohl A. 2009. Asymmetries in the moisture origin of Antarctic precipitation. *Geophysical Research Letters* **36**: L22803, doi: 10.1029/2009gl040242.

Sodemann H, Schwierz C, Wernli H. 2008. Interannual variability of Greenland winter precipitation sources: Lagrangian moisture diagnostic and North Atlantic Oscillation influence. *Journal of Geophysical Research-Atmospheres* **113**: D03107, doi: 10.1029/2007jd008503.

Stohl A, James P. 2004. A Lagrangian analysis of the atmospheric branch of the global water cycle. Part I: method description, validation, and demonstration for the August 2002 flooding in central Europe. *Journal of Hydrometeorology* **5**: 656–678.

Stohl A, James P. 2005. A Lagrangian analysis of the atmospheric branch of the global water cycle. Part II: moisture transports between earth's ocean basins and river catchments. *Journal of Hydrometeorology* **6**: 961–984.

Stohl A, Forster C, Sodemann H. 2008. Remote sources of water vapor forming precipitation on the Norwegian west coast at 60 degrees N – a tale of hurricanes and an atmospheric river. *Journal of Geophysical Research-Atmospheres* **113**: D05102, doi: 10.1029/2007jd009006.

Sun B, Wang HJ. 2014. Moisture sources of Semiarid Grassland in China using the Lagrangian particle model FLEXPART. *Journal of Climate* **27**: 2457–2474.

Trenberth KE, Dai A, Rasmussen RM, Parsons DB. 2003. The changing character of precipitation. *Bulletin of the American Meteorological Society* **84**: 1205–1217.

Weyhenmeyer CE, Burns SJ, Waber HN, Macumber PG. 2002. Isotope study of moisture sources, recharge areas, and groundwater flow paths within the eastern Batinah coastal plain, Sultanate of Oman. *Water Resources Research* **38**: 2-1–2-22, doi: 10.1029/2000wr000149.

Xu XD, Miao QJ, Wang JZ, Zhang XJ. 2003. The water vapor transport model at the regional boundary during the Meiyu period. *Advances in Atmospheric Sciences* **20**: 333–342.

Zhou YS, Gao ST, Deng G. 2005. A Diagnostic study of water vapor transport and budget during heavy precipitation over the Changjiang River and the Huaihe River Basins in 2003. *Chinese Journal of Atmospheric Sciences* **29**: 195–204 (in Chinese).

